

# Achieving Heisenberg scaling by probe-ancilla interaction in quantum metrology

Jingyi Fan<sup>1</sup> and Shengshi Pang<sup>1\*</sup>

*School of Physics, Sun Yat-sen University, Guangzhou, Guangdong 510275, China*

The Heisenberg scaling is an ultimate precision limit of parameter estimation allowed by the principles of quantum mechanics, with no counterpart in the classical realm, and has been a long-pursued goal in quantum metrology. It has been known that interactions between the probes can help reach the Heisenberg scaling without entanglement. In this work, we show that interactions between the probes and the additional dimensions of an ancillary system may also increase the precision of parameter estimation to surpass the standard quantum limit and attain the Heisenberg scaling without entanglement, if the measurement scheme is properly designed. The quantum Fisher information exhibits periodic patterns over the evolution time, implying the existence of optimal time points for measurements that can maximize the quantum Fisher information. By implementing optimizations over the Hamiltonian, the initial states of the probes and the ancillary system, the interaction strength and the time points for measurements, our protocol achieves the Heisenberg scaling for the parameter of the probe Hamiltonian, in terms of both evolution time and probe number. Our protocol features in two aspects: (i) the Heisenberg scaling can be achieved by a product state of the probes, (ii) mere local measurement on the ancilla is sufficient, both of which reduce the quantum resources and the implementation complexity to achieve the Heisenberg scaling.

## I. INTRODUCTION

The pursuit of precision in measurements is a long-standing goal in physics and other fields and has been extensively studied in the science of metrology. Quantum metrology, the extension of metrology to the quantum regime, aims to push the measurement precision to the ultimate limit constrained by the intrinsic statistical uncertainty introduced by quantum mechanics. A fundamental limit in quantum metrology is the standard quantum limit on the errors of parameter estimation by measurements of uncorrelated systems, which scales linearly with  $N^{-1/2}$  with  $N$  the total number of measurements. The standard quantum limit is essentially rooted in the central limit theorem of classical statistics [1]. In contrast, if non-classical resources such as quantum entanglement and quantum squeezing [2, 3] are introduced to the systems, the sensitivity of quantum measurements can be enhanced and the precision limit of parameter estimation may surpass the standard quantum limit and reach the Heisenberg limit. The Heisenberg limit is a precision scaling of parameter estimation inverse to the evolution time or the number of probes, much lower than the standard quantum limit with no counterpart in classical physics. This advancement has led to substantial progress in quantum metrology [4], both theoretically and experimentally, as reported in previous literatures concerning typical tasks such as phase estimation [5–8] and more recently focused on multi-parameter estimation [9–11], etc. Besides, quantum metrology has been applied in a variety of areas such as atomic clocks [12–14], gravitational wave sensing [15, 16], dark matter [17, 18], biological sensing [19] and quantum imaging [9, 20–23], revolutionizing our ability to collect information on physical quantities and parameters with high precision.

Parameter estimation is a fundamental component of quantum metrology, as it offers the appropriate tools and methods to develop quantum measurement schemes that achieve high precision [24–26]. In classical parameter estimation, the inference of unknown parameters relies on parameter-dependent probability distributions. The Cramér-Rao bound sets a lower limit on the variance of parameter estimation over all estimation strategies, which turns out to be determined by the inverse of the Fisher information [24]. In the quantum regime, the parameters of interest are usually encoded into the quantum state of the system. The quantum Fisher information, defined as the maximum Fisher information over all possible generalized measurements, gives the quantum Cramér-Rao bound for quantum parameter estimation. In addition, quantum estimation protocols can take advantage of quantum mechanical features, such as non-classical properties of quantum states, which offer enhanced sensing capability compared to classical methods.

In quantum metrology, the parameters of interest are often associated with quantum dynamics, and the primary goal is to design measurement strategies that achieve the highest precision. A general approach is to encode the parameters of interest into the probe system through an associated quantum dynamical evolution, and then to measure the evolved system and estimate the parameters through processing the measurement outcomes [27, 28]. To maximize the information of the parameters that can be extracted from the evolved probe system, it is essential to optimize both the state of the probe system and the measurement strategies, as they significantly influence the precision of the estimation [29, 30]. In addition to these quantum metrology protocols, the sensitivity of the precision can also be enhanced by utilizing appropriate interactions [31, 32], introducing quantum controls [33–36], etc. With appropriate initial states and measurement strategies, the precision limit can exceed the standard quantum limit and achieve the Heisenberg

\* pangshsh@mail.sysu.edu.cn

scaling for typical tasks of quantum parameter estimation such as phase estimation [27].

In practical scenarios, the environment-induced noise can undermine the advantage of quantum metrology and prevents measurements from attaining the Heisenberg limit, even reducing it to the standard quantum limit [37–41]. In the presence of noise, the finite coherence time reduces the period during which the quantum states can maintain the superposition and the quantum Fisher information can increase, suggesting the importance of choosing appropriate time points for measurements to extract as much information as possible from noisy quantum systems, which is essential for the design of robust quantum parameter estimation strategy against environmental noises. The pursuit of measurement precision that exceeds the standard quantum limit has led to the development of a variety of ingenious strategies, including the use of squeezed states [2, 3, 42–45], ancillary systems [31, 32, 46, 47], the exploitation of the time-reversal procedure [48–51] and non-Markovian effects [52–54], etc.

A general approach of quantum metrology is illustrated in Fig. 1a, which involves preparing the probes in a proper initial state, encoding the parameters of interest through a unitary transformation, performing measurements on the final state, and processing the outcomes by proper estimation strategies to infer the unknown parameters. Typical quantum protocols include the utilization of quantum resources like entangled states to enhance the measurement sensitivity. To date, the multi-particle entanglement has been realized in various many-body quantum systems [55–59], leading to enhanced measurement precision [60–62]. Nevertheless, the use of quantum entanglement often involves the challenges regarding the cost, efficiency, and quality in their preparation and application. As the size of the system scales up, the quantum resources become increasingly delicate and fragile against environmental noise, which can disrupt the non-classical characteristics of the quantum systems even if the noise is weak. Such vulnerability gives rise to significant decoherence in quantum states, resulting in the loss of quantum entanglement and the return to classical behavior of quantum systems [63–65].

In recent years, interactions have been found useful in quantum metrology to achieve or even beat the Heisenberg limit [66], without the assistance of quantum entanglement, circumventing the difficulties of preparing quantum correlated states. It is shown that  $k$ -body interactions between the probes can increase the precision of quantum parameter estimation beyond the Heisenberg scaling and push the precision limit to a super-Heisenberg scaling  $N^{-k}$  [31, 47, 67]. Such interaction-based super-Heisenberg scalings have been realized by experiments [68, 69].

Inspired by the previous literatures on interaction-based quantum metrology, in this work, we propose a simple but non-trivial metrological protocol that does not require interaction or entanglement between the probes but introduces ancillary system to interact with them.

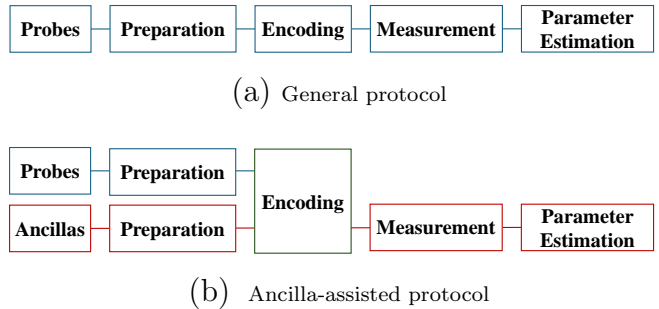


Figure 1: Schematic diagrams outlining a general quantum metrology protocol and the current ancilla-assisted protocol, both including preparing quantum probes in a desired initial state, allowing the probes to evolve to encode the parameters of interest, and extracting the information of the parameters from the measurements. (a) The general protocol takes advantage of quantum resources such as entanglement and squeezed states to raise the measurement precision beyond the standard quantum limit approaching the Heisenberg scaling. (b) An alternative protocol using ancillas and uncorrelated probes employs probe-ancilla interaction to achieve the Heisenberg scaling without entanglement. This protocol also simplifies the measurement process by observing the ancillas only.

The interaction between the ancillary system and the probe system is mediated by a two-body coupling Hamiltonian, which can be experimentally realized in a variety of quantum systems including trapped ions [70–72], superconducting circuits [73–76], etc. We show that such two-body interaction between the ancillary system and the probe system can lead to enhanced precision that surpasses the standard quantum limit in estimating the parameters of the probes, and the measurement to realize such enhanced precision just needs to be local on the ancillary system, without the necessity of nonlocal measurements as in general quantum metrological protocols. Additionally, the quantum Fisher information of the evolved ancillary system exhibits periodic patterns over the evolution time. In order to achieve the highest precision, optimizations are required on the tailoring of the Hamiltonian, the time points for measurements, and the tuning of the interaction strength between the ancillary system and the probe system. By implementing these optimizations, the precision of the protocol can achieve the Heisenberg scaling at those periodic time points, in terms of both evolution time and probe number. The whole protocol is illustrated in Fig. 1b.

The paper is organized as follows. In Sec. II, we give preliminaries for the general theory of parameter estimation in quantum metrology. In Sec. III, we introduce the general framework for our metrology protocol. Optimizations of the initial states of both the ancilla and the probe system, the Hamiltonian, the time points for measurements and the interaction strength are investigated,

and the highest precision of the protocol is derived in Sec. IV. Finally the paper is concluded in Sec. V.

## II. PRELIMINARIES

In this section, we provide a concise overview of the fundamental concepts in quantum metrology relevant to the current research.

In quantum metrology, the key task is to improve the estimation precision for unknown parameters in quantum systems. Enhanced sensitivity can be achieved if typical quantum resources, such as entanglement and squeezed states, are utilized. The unknown parameters are encoded into the state of some probes by quantum processes dependent on those parameters. Subsequently, appropriate measurements are performed on the probes, and the measurement outcomes are analyzed by sophisticated statistical strategies to infer the unknown parameters.

The theory of quantum parameter estimation is rooted in the classical theory of parameter estimation. In the classical parameter estimation, the goal is to estimate an unknown parameter  $\theta$  from a  $\theta$ -dependent probability distribution  $p(x|\theta)$  of a random variable  $x$ . The mean squared error of the estimator  $\hat{\theta}$  is limited by the Cramér–Rao bound [77],

$$\mathbb{E}[(\hat{\theta} - \theta)^2] \geq (NF)^{-1} + \mathbb{E}[(\hat{\theta} - \theta)]^2, \quad (1)$$

where the first term at the right side is the lower bound of the variance of the estimation and the second term is the systematic error of the estimation,  $N$  is the number of measurement repetitions, and  $F$  represents the Fisher information, defined as

$$F = \int \frac{[\partial_\theta p(x|\theta)]^2}{p(x|\theta)} dx. \quad (2)$$

When the parameter estimation theory is applied to the quantum realm, the parameter of interest is usually encoded in a quantum state, and the choice of measurement basis can significantly influence the distribution of measurement outcomes and change the precision of parameter estimation. The quantum Cramér–Rao bound, derived by minimizing the variance of estimation over all possible measurement bases, gives the lowest achievable variance for any estimation strategy. This extends the classical Fisher information to the quantum Fisher information which quantifies the sensitivity of parameter estimation in quantum systems.

For an unknown parameter  $\theta$  in a density matrix  $\rho_\theta$ , the quantum Fisher information can be derived as

$$F_Q = \text{Tr}(\rho_\theta L_\theta^2), \quad (3)$$

where the Hermitian operator  $L_\theta$  is the symmetric logarithmic derivative with respect to the parameter  $\theta$  [25], determined by

$$\partial_\theta \rho_\theta = \frac{1}{2}(\rho_\theta L_\theta + L_\theta \rho_\theta). \quad (4)$$

Consider an initial state with a spectral decomposition  $\rho = \sum_i p_i |\lambda_i\rangle\langle\lambda_i|$ , the quantum Fisher information can be explicitly derived as

$$F_Q = \sum_{\lambda_i + \lambda_j \neq 0} \frac{2|\langle\lambda_i|\partial_\theta \rho_\theta|\lambda_j\rangle|^2}{\lambda_i + \lambda_j}. \quad (5)$$

For a pure state  $\rho_\theta = |\psi_\theta\rangle\langle\psi_\theta|$ , the quantum Fisher information (5) is reduced to

$$F_Q = 4 \left[ \langle\partial_\theta \psi_\theta|\partial_\theta \psi_\theta\rangle - |\langle\psi_\theta|\partial_\theta \psi_\theta\rangle|^2 \right], \quad (6)$$

with  $|\partial_\theta \psi_\theta\rangle = \partial|\psi_\theta\rangle/\partial\theta$ . Furthermore, for a quantum system evolved from a pure state  $|\psi_0\rangle$  under a  $\theta$ -dependent Hamiltonian  $H_\theta$  for time  $t$ , the quantum Fisher information can be further simplified to

$$F_Q = 4t^2 \langle\Delta^2 H_\theta\rangle, \quad (7)$$

where  $\langle\Delta^2 H_\theta\rangle$  is the variance of  $H_\theta$  for the initial state  $|\psi_0\rangle$ , given as

$$\langle\Delta^2 H_\theta\rangle = \langle\psi_0|H_\theta^2|\psi_0\rangle - \langle\psi_0|H_\theta|\psi_0\rangle^2. \quad (8)$$

A simple and typical scenario of quantum metrology considers a probe with a Hamiltonian  $H_\theta = \theta\tilde{H}$ . The maximal quantum Fisher information for the parameter  $\theta$  can be obtained as

$$\max_{|\psi_0\rangle} F_Q = t^2 (\lambda_{\max} - \lambda_{\min})^2, \quad (9)$$

when

$$|\psi_0\rangle = (|\lambda_{\max}\rangle + |\lambda_{\min}\rangle)/\sqrt{2}, \quad (10)$$

where  $\lambda_{\max}$  and  $\lambda_{\min}$  are the maximum and minimum eigenvalues of the Hamiltonian  $\tilde{H}$ , corresponding to eigenstates  $|\lambda_{\max}\rangle$  and  $|\lambda_{\min}\rangle$ .

For a system of  $N$  probes, if the probes are uncorrelated, the maximal quantum Fisher information is

$$\max_{|\psi_0\rangle} F_Q = Nt^2 \left( \lambda_{\max}^{(i)} - \lambda_{\min}^{(i)} \right)^2, \quad (11)$$

with the initial state

$$|\psi_0\rangle = (|\lambda_{\max}\rangle + |\lambda_{\min}\rangle)^{\otimes N} / \sqrt{2}, \quad (12)$$

according to the additivity of quantum Fisher information for uncorrelated systems [6], implying the measurement precision scales as  $\Delta\theta \propto 1/\sqrt{N}$ , which is the standard quantum limit. However, by employing a maximally entangled state

$$|\psi_0\rangle = (|\lambda_{\max}\rangle^{\otimes N} + |\lambda_{\min}\rangle^{\otimes N}) / \sqrt{2}, \quad (13)$$

the maximal quantum Fisher information becomes

$$\max_{|\psi_0\rangle} F_Q = N^2 t^2 \left( \lambda_{\max}^{(i)} - \lambda_{\min}^{(i)} \right)^2, \quad (14)$$

indicating that the standard quantum limit can be surpassed [78] and higher precision is attained by the measurements, and the corresponding measurement precision scales as  $\Delta\theta \propto 1/N$ , which is the Heisenberg scaling, a  $\sqrt{N}$  improvement over the standard quantum limit.

The simplest scenario involves a two-level system, for which the Bloch representation is employed to depict the quantum state, which can be represented by  $\rho_\theta = \frac{1}{2}(I + \mathbf{r}_\theta \cdot \boldsymbol{\sigma})$ , where  $\mathbf{r}_\theta = [x_\theta, y_\theta, z_\theta]$  is the Bloch vector satisfying  $|\mathbf{r}_\theta|^2 \leq 1$ , and  $\boldsymbol{\sigma} = [\sigma_x, \sigma_y, \sigma_z]$  is the vector of the Pauli matrices. For a two-level system, the quantum Fisher information can then be written as

$$F_Q = |\partial_\theta \mathbf{r}_\theta|^2 + \frac{(\mathbf{r}_\theta \cdot \partial_\theta \mathbf{r}_\theta)^2}{1 - |\mathbf{r}_\theta|^2}, \quad (15)$$

where  $|\cdot|$  denotes the Euclidean norm of a vector. The Bloch representation, compared with Eq.(5), is a convenient tool as it obviates the need for spectral decomposition of the density matrix, a process that can be resource-consuming and hard to tackle for high-dimensional systems.

### III. HAMILTONIANS AND DYNAMICS OF ANCILLARY SYSTEM

In this work, we consider a scenario where an ancillary system is introduced to interact with the probes and investigate its effect in enhancing the sensitivity of measurement. The general Hamiltonian for the probe system and the ancillary system involving the free Hamiltonian  $H_0$  and interaction Hamiltonian  $H_I$  can be written as

$$H_{tot} = H_0 + H_I = \omega H_p + \omega_a H_a + gB \otimes A, \quad (16)$$

where  $H_p$  and  $H_a$  are the free Hamiltonians of the probe system and the ancillary system,  $\omega_a$  is the frequency of the ancillary system, and  $\omega$  is the frequency of the probe system which is supposed to be the unknown parameter to estimate. The interaction Hamiltonian  $H_I$  describes the coupling between the two systems with the strength  $g$ , where  $B$  and  $A$  are the observables of the probe system and the ancillary system respectively.

The goal is to measure the parameter  $\omega$  of the Hamiltonian  $H_p$  in the probe system. Suppose the initial density matrix can be factorized between the probe system and ancillary system,  $\rho_{pa}(0) = \rho_p(0) \otimes \rho_a(0)$ . The joint evolution of the probe system and the ancillary system can be written as

$$\rho_{pa}(t) = U(t) \rho_p(0) \otimes \rho_a(0) U^\dagger(t), \quad (17)$$

where  $U(t) = e^{-iH_{tot}t}$  is the unitary dynamical evolution under the total Hamiltonian (16) encoding the parameter  $\omega$  into the evolved state.

As we focus on local measurements on the ancillary system alone in this work, the probe system can be traced

out from the joint density matrix (17), and the reduced evolution of the ancillary system can be written as

$$\rho_a(t) = \text{Tr}_p[\rho_{pa}(t)]. \quad (18)$$

As the reduced density matrix  $\rho_a(t)$  is dependent on the unknown parameter  $\omega$ , the information of the parameter  $\omega$  can be obtained through the measurements on the ancillary system. The precision of estimating the parameter  $\omega$  can be determined by the quantum Fisher information for a general mixed state (5). When the ancilla is a two-dimensional system, the quantum Fisher information can be simplified in the Bloch representation (15).

### IV. OPTIMIZATIONS OF QUANTUM FISHER INFORMATION

In quantum metrology, the parameter of interest is inferred from the evolved state of the system and the evolved state of the system generally depends on the initial state of the system and the evolution path under the Hamiltonian, so proper optimizations of the initial state and the Hamiltonian are vital to the performance of precision measurements.

In this section, we investigate the optimizations of the estimation precision over the initial state and the Hamiltonian of the probes and the ancillary system, and show that such optimizations can significantly increase the estimation precision. In particular, when there are multiple probes present for sensing the frequency, proper optimizations of the interaction Hamiltonian between the probes and the ancillary system can raise the precision limit to the Heisenberg scaling even when the probes are initially in a product state, which manifests the power of interaction between the probes and the external degrees of freedom introduced by the ancilla, in addition to the known advantage of interaction within the probes [31, 47, 66–68].

#### A. Optimization of ancilla state

A proper initial state is crucial to enhancing the precision of parameter estimation for quantum system. While the probe system is generally considered to have arbitrary dimensions, only the highest and the lowest levels of the system will be involved in determining the maximal Fisher information [27]. Hence, we use two-level systems to simulate the probes in this work. For simplicity, we also assume the ancillary system to be two-level, which is not necessarily the optimal choice but will be shown to be sufficient to attain the Heisenberg scaling. For the convenience of computation, we choose the observable  $A$  of the ancillary system in the interaction Hamiltonian to commute with the free Hamiltonian  $H_a$  of the ancillary system, i.e.,  $[H_a, A] = 0$ . This allows  $H_a$  and  $A$  to share a set of common eigenstates  $|a_k\rangle$ ,  $k = 1, 2$ , associated with eigenvalues  $h_k$  and  $a_k$ , respectively.

Suppose the ancillary system is initialized in a pure state,

$$|\psi_a\rangle = \cos\alpha|a_1\rangle + e^{-i\phi}\sin\alpha|a_2\rangle. \quad (19)$$

Its reduced density matrix after an evolution under the total Hamiltonian (16) for time  $t$  is given by

$$\rho_a(t) = \text{Tr}_p [e^{-iH_{tot}t}\rho_p(0) \otimes |\psi_a\rangle\langle\psi_a|e^{iH_{tot}t}]. \quad (20)$$

Since the eigenstates  $|a_1\rangle$  and  $|a_2\rangle$  of the ancillary system are orthogonal, the final density matrix of the ancillary system can also be represented by a Bloch vector  $\mathbf{r} = [r_x, r_y, r_z]$ , which can be derived as

$$r_x = \sin(2\alpha)(\Gamma_r \cos(\phi) - \Gamma_i \sin(\phi)), \quad (21)$$

$$r_y = -\sin(2\alpha)(\Gamma_r \sin(\phi) + \Gamma_i \cos(\phi)), \quad (22)$$

$$r_z = \cos(2\alpha), \quad (23)$$

where  $\Gamma_r$  and  $\Gamma_i$  are the real and imaginary components of the function

$$\Gamma(t) = \langle\psi_p|e^{it\Theta_2^\dagger}e^{-it\Theta_1}|\psi_p\rangle. \quad (24)$$

Here  $|\psi_p\rangle$  denotes the initial state of the probe system and the operator  $\Theta_k$  is defined as

$$\Theta_k = \omega H_p + \omega_a h_k I + g a_k B, \quad (25)$$

satisfying the relation

$$H_{tot}(|\psi_p\rangle \otimes |a_k\rangle) = (\Theta_k|\psi_p\rangle) \otimes |a_k\rangle, \quad (26)$$

since  $|a_k\rangle$  is the eigenstate of both  $H_a$  and  $A$ , therefore, we have

$$e^{-itH_{tot}}|\psi_p\rangle \otimes |a_k\rangle = e^{-it\Theta_k}|\psi_p\rangle \otimes |a_k\rangle. \quad (27)$$

The quantum Fisher information can hence be written in the Bloch representation,

$$F_Q = \sin^2(2\alpha) \frac{(\partial_\omega \Gamma_r)^2 + (\partial_\omega \Gamma_i)^2 - (\Gamma_r \partial_\omega \Gamma_r - \Gamma_i \partial_\omega \Gamma_i)^2}{1 - \Gamma_r^2 - \Gamma_i^2}. \quad (28)$$

where  $\partial_\omega$  denotes the derivative with respect to the estimated parameter  $\omega$ . It is obvious that the optimal  $\alpha$  of the initial state of the ancillary system that maximizes the quantum Fisher information  $F_Q$  is  $\alpha = \pi/4$ . Furthermore, as Eq. (28) is independent of  $\phi$ , we set the azimuthal angle  $\phi$  to be zero and then the optimal initial state of the ancillary system is given by

$$|\psi_a\rangle = \frac{1}{\sqrt{2}}|a_1\rangle + \frac{1}{\sqrt{2}}|a_2\rangle. \quad (29)$$

By employing the optimal initial state of the ancillary system, the quantum Fisher information (28) can be simplified as

$$F_Q(t) = |\partial_\omega \Gamma(t)|^2 + \frac{1}{4} \frac{(\partial_\omega |\Gamma(t)|^2)^2}{1 - |\Gamma(t)|^2}. \quad (30)$$

According to Eq. (30), the time scaling of the quantum Fisher information is determined by  $\partial_\omega \Gamma(t)$  and  $\partial_\omega |\Gamma(t)|^2$ . Specifically, the derivative of the function  $\Gamma(t)$  with respect to  $\omega$  is related to the derivative of the operator  $e^{-it\Theta_k}$  with respect to  $\omega$ , which can be worked out as

$$\partial_\omega e^{-it\Theta_k} = -i \int_0^t e^{-i(t-\tau)\Theta_k} (\partial_\omega \Theta_k) e^{-i\tau\Theta_k} d\tau \quad (31)$$

$$= -ie^{-it\Theta_k} \int_0^t e^{i\tau\Theta_k} H_p e^{-i\tau\Theta_k} d\tau. \quad (32)$$

By utilizing the spectral decomposition of  $\Theta_k$ ,  $\Theta_k = \sum_i \lambda_i^{(k)} |\lambda_i^{(k)}\rangle\langle\lambda_i^{(k)}|$ , the integration over the equal eigenvalues of  $\Theta_k$  may result in a linear term with the evolution time  $t$  while integrating over  $\Theta_k$ 's unequal eigenvalues yields a constant-order term,

$$\begin{aligned} & \int_0^t e^{i\tau\Theta_k} H_p e^{-i\tau\Theta_k} d\tau \\ &= t \sum_{\lambda_i^{(k)}=\lambda_j^{(k)}} |\lambda_i^{(k)}\rangle\langle\lambda_i^{(k)}| H_p |\lambda_j^{(k)}\rangle\langle\lambda_j^{(k)}| + O(1). \end{aligned} \quad (33)$$

Consequently, the term  $\partial_\omega \Gamma(t)$  exhibits linear scaling behavior with respect to the evolution time  $t$ , that is  $\partial_\omega \Gamma(t) \propto t$ , if the linear term in Eq. (33) does not vanish. Substituting this result to Eq. (30), we arrive at the Heisenberg scaling of the quantum Fisher information  $F_Q$  with respect to time,  $F_Q(t) \propto t^2$ .

So far, we have seen the possibility that the quantum Fisher information achieves the Heisenberg scaling with respect to the evolution time by employing the optimal initial state of the ancillary system. Nevertheless, the Heisenberg scaling in terms of the total probe number is more involved which is influenced by both the initial state of the probe system and the interaction term. Details will be investigated in the following subsection, where the condition for the Heisenberg scaling with respect to the evolution time will also be elaborated.

## B. Configuration of probe system

In order to present a detailed and quantitative condition for the Heisenberg scaling with respect to the number of probes, we consider a system composed of  $N$  identical probes, which are uncorrelated before the unitary evolution under the Hamiltonian. In this case, the  $N$ -probe state is  $|\psi_p\rangle = |\phi_p^{(1)}\rangle \otimes |\phi_p^{(2)}\rangle \otimes \dots \otimes |\phi_p^{(N)}\rangle$ , where  $|\phi_p^{(k)}\rangle$  represents the initial state of the  $k$ -th probe. Similarly, the dynamical evolution can be decomposed into one-body evolutions acting on each probe individually.

Suppose each individual probe of the probe system is initially in the same state  $|\phi_p\rangle$  and the Hamiltonian can be written by the vector of Pauli matrices  $\boldsymbol{\sigma}$  as

$$H_p = \sum_i \mathbf{m} \cdot \boldsymbol{\sigma}^{(i)}, \quad B = \sum_i \mathbf{n} \cdot \boldsymbol{\sigma}^{(i)}, \quad (34)$$

with  $\mathbf{m} = (m_x, m_y, m_z) \in \mathbb{R}^3$  and  $\mathbf{n} = (n_x, n_y, n_z) \in \mathbb{R}^3$ . Consequently, the  $N$ -body operator  $\Theta_k$  25 can be represented by the Kronecker sum of one-body operators  $\vartheta_k^{(i)}$ , i.e.,  $\Theta_k = \oplus_i \vartheta_k^{(i)}$ , where

$$\vartheta_k^{(i)} = \lambda \omega \mathbf{m} \cdot \boldsymbol{\sigma}^{(i)} + \frac{\omega_a}{N} h_k I_2 + g a_k \mathbf{n} \cdot \boldsymbol{\sigma}^{(i)}. \quad (35)$$

Here  $\lambda$  can be considered as the difference between the maximal and the minimal levels of a single probe, which is currently simulated by a two-level system. The operator  $\vartheta_k^{(i)}$  is identical for each probe, and we denote them as  $\vartheta_k$  for simplicity in the following if no ambiguity occurs. Similar to the definition and relation of  $\Theta_k$  presented in Eq. (25) and Eq. (27), the one-body operator  $\vartheta_k$  satisfies the relation

$$e^{-itH_{tot}} |\psi_p\rangle \otimes |a_k\rangle = (e^{-it\vartheta_k} |\phi_p\rangle)^{\otimes N} \otimes |a_k\rangle. \quad (36)$$

We can therefore define the function  $\gamma(t)$  for a single probe by the one-body operator  $\vartheta_k$  and the initial state of each probe  $|\phi_p\rangle$  as

$$\gamma(t) = \langle \phi_p | e^{it\vartheta_2} e^{-it\vartheta_1} | \phi_p \rangle, \quad (37)$$

satisfying

$$\Gamma(t) = \gamma(t)^N, \quad (38)$$

$$\partial_\omega \Gamma(t) = N \gamma(t)^{N-1} \partial_\omega \gamma(t). \quad (39)$$

The quantum Fisher information can then be written in terms of the function  $\gamma(t)$ ,

$$F_Q(t) = N^2 |\gamma(t)|^{2N-2} |\partial_\omega \gamma(t)|^2, \quad (40)$$

which involves a quadratic factor of  $N$  that is necessary to the Heisenberg scaling of the quantum Fisher information with respect to the total number  $N$  of the probes.

However, the absolute value of the function  $\gamma(t)$ , i.e.,  $|\gamma(t)|$ , can range between 0 and 1 by the definition (37) since the dynamical operators  $e^{-it\vartheta_k}$  are unitary. If  $|\gamma(t)| \neq 1$ , the term  $|\gamma(t)|^{2N-2}$  will result in an exponential decay of  $F_Q(t)$  with respect to  $N$  when  $N$  is large, and the quantum Fisher information will be diminished in this case. So it is critical to guarantee  $|\gamma(t)| = 1$  by proper optimizations over the initial states and the Hamiltonians of the probes and the ancillary system in order to realize the Heisenberg scaling. This will be investigated in detail in the next subsection.

### C. Optimization of time points and probe state

The quantum Fisher information has a periodic pattern with respect to the evolution time  $t$  originated from the periodic structure of  $\gamma(t)$  (37) which determines the quantum Fisher information by Eq. (40). This will be made clearer later in this subsection. So, we just need to consider the scaling of the quantum Fisher information

with respect to the specific time points that extremize the quantum Fisher information, and the measurements on the ancillary system can be performed at those time points. Furthermore, the initial state of the probe system, denoted by  $|\phi_p\rangle$ , can also significantly affect the quantum Fisher information. It will be shown that by optimizing the initial state of the probe system and selecting appropriate time points for measurements, it is possible to achieve the Heisenberg scaling of the quantum Fisher information with respect to time at those time points.

By the Bloch representation of the initial probe state,

$$|\phi_p\rangle \langle \phi_p| = \frac{1}{2} (I + \mathbf{v} \cdot \boldsymbol{\sigma}), \quad \mathbf{v} = (v_x, v_y, v_z) \in \mathbb{R}^3, \quad (41)$$

with  $|\mathbf{v}| = 1$  for a pure state, the function  $\gamma(t)$  can be written as

$$\gamma(t) = e^{-it\omega_a \frac{h_1 - h_2}{N}} [\gamma_r(t) + i\gamma_i(t)], \quad (42)$$

where

$$\begin{aligned} \gamma_r(t) &= \cos(\mu_1 t) \cos(\mu_2 t) \\ &+ \frac{\mu_1^2 + \mu_2^2 - g^2 (a_1 - a_2)^2}{2\mu_1 \mu_2} \sin(\mu_1 t) \sin(\mu_2 t), \end{aligned} \quad (43)$$

$$\gamma_i(t) = \mathbf{k}(t) \cdot \mathbf{v}, \quad (44)$$

and

$$\mathbf{k}(t) = c_m \mathbf{m} + c_n \mathbf{n} + c_{mn} \mathbf{m} \times \mathbf{n}, \quad (45)$$

with

$$c_m = \left[ \frac{\cos(\mu_1 t) \sin(\mu_2 t)}{\mu_2} - \frac{\sin(\mu_1 t) \cos(\mu_2 t)}{\mu_1} \right] \lambda \omega, \quad (46)$$

$$c_n = \left[ \frac{a_2 \sin(\mu_2 t) \cos(\mu_1 t)}{\mu_2} - \frac{a_1 \sin(\mu_1 t) \cos(\mu_2 t)}{\mu_1} \right] g, \quad (47)$$

$$c_{mn} = \frac{\sin(\mu_1 t) \sin(\mu_2 t)}{\mu_1 \mu_2} (a_1 - a_2) g \lambda \omega. \quad (48)$$

Specifically,  $\gamma_r(t)$  and  $\gamma_i(t)$  denote the real and imaginary components of the function  $\gamma(t)$ , respectively, up to the global phase  $e^{-it\omega_a \frac{h_1 - h_2}{N}}$  which is irrelevant to the quantum Fisher information. Here the functions  $\mu_k$  are defined as

$$\mu_k = \sqrt{a_k^2 g^2 + 2a_k g \lambda \omega \mathbf{m} \cdot \mathbf{n} + \lambda^2 \omega^2}, \quad k = 1, 2, \quad (49)$$

describing the frequencies of the periodic behavior of the function  $\gamma(t)$ , which determines the periodic nature of the evolution of the quantum Fisher information.

The quantum Fisher information (40) indicates that the exponential decay may substantially counteract the Heisenberg scaling. However, if  $|\gamma(t)| = 1$ , the exponential decay vanishes, allowing for the achievement of the

Heisenberg scaling in terms of the total probe number  $N$ , so it is crucial to have  $|\gamma(t)| = 1$ . In the following, we will explore the condition to achieve this maximum value of  $|\gamma(t)|$ .

The absolute value of the function  $\gamma(t)$ , which is determined by the vector  $\mathbf{v}$ , can be given by

$$|\gamma(t)|^2 = \gamma_r^2(t) + \gamma_i^2(t) = \gamma_r^2(t) + (\mathbf{k}(t) \cdot \mathbf{v})^2. \quad (50)$$

In general, when  $\gamma_r(t)$  and  $\mathbf{k}(t)$  are fixed, both of which are determined by  $\mu_1, \mu_2$ , the maximal  $\mathbf{k}(t) \cdot \mathbf{v}$  over all possible  $\mathbf{v}$  leads to the maximum value of  $|\gamma(t)|^2$ . And  $\mathbf{k}(t) \cdot \mathbf{v}$  is maximized when  $\mathbf{v}$  is parallel or antiparallel to  $\mathbf{k}(t)$  considering  $|\mathbf{v}| = 1$  for the pure initial state  $|\psi_p\rangle$ , leading to  $\mathbf{k}(t) \cdot \mathbf{v} = \pm |\mathbf{k}(t)|$  at the optimal time points. However, since the initial state of the probe system does not change over time, this maximum value can be achieved only at those optimized time points  $t_p$ , and the optimal vector  $\mathbf{v}$  can be obtained at the optimized time points  $t_p$  by

$$\mathbf{v} = \frac{\mathbf{k}(t_p)}{|\mathbf{k}(t_p)|}. \quad (51)$$

It can be verified by Eq. (43) and (45) that for all time  $t$ ,

$$\gamma_r^2(t) + |\mathbf{k}(t)|^2 = 1. \quad (52)$$

So when the time points are optimized,  $|\gamma(t_p)| = 1$ , considering Eq. (50) and  $\mathbf{k}(t_p) \cdot \mathbf{v} = \pm |\mathbf{k}(t_p)|$ . This yields the maximum value of  $|\Gamma(t)|^2$  at the optimized time points  $t_p$ ,

$$|\Gamma(t_p)|^2 = |\gamma(t_p)|^{2N} = 1. \quad (53)$$

A further simplification can be achieved by representing the function  $\gamma(t)$  by its amplitude  $|\gamma(t)|$  and argument  $\theta(t)$ , where

$$\theta(t) = \arctan \frac{\text{Im}[\gamma(t)]}{\text{Re}[\gamma(t)]} = \arctan \frac{\gamma_i(t)}{\gamma_r(t)}. \quad (54)$$

As  $|\gamma(t_p)| = 1$  at the optimal time points  $t_p$ ,  $\gamma(t_p)$  can be written as  $\gamma(t_p) = \exp[i\theta(t_p)]$ . So, the quantum Fisher information at the time points  $t_p$  can then be given in a simpler manner,

$$F_Q(t_p) = N^2 |\partial_\omega \theta(t_p)|^2 = N^2 \left( \frac{\partial_\omega \gamma_i(t_p)}{\gamma_r(t_p)} \right)^2, \quad (55)$$

which manifests the Heisenberg scaling in terms of the total probe number  $N$ . Moreover, the Heisenberg scaling in terms of the optimal time points  $t_p$  can also be derived from Eq. (55) as the derivative of  $\gamma_i(t_p)$  with respect to  $\omega$  involves the derivatives of the sine and cosine functions of  $\mu_1 t$  and  $\mu_2 t$  which gives a linear term of  $t_p$  multiplied by some coefficient. That coefficient can be further optimized, and the quantum Fisher information (55) reaches the maximum when both cosine functions,  $\cos(\mu_1 t)$  and

$\cos(\mu_2 t)$ , are equal 1 simultaneously. In this case, we have  $\gamma_i(t_p) = 0$  as  $\mathbf{k}(t_p) = 0$ , and thus  $\gamma_r(t_p) = 1$  as  $|\gamma(t)| = 1$  at the optimal time points. And the quantum Fisher information (55) can be simplified to

$$F_Q(t_p) = N^2 (\partial_\omega \gamma_i(t_p))^2. \quad (56)$$

Note that

$$\partial_\omega \theta(t_p) = \partial \gamma_i(t_p) = \partial_\omega \mathbf{k}(t_p) \cdot \mathbf{v}, \quad (57)$$

so the further optimization of the initial state  $|\psi_p\rangle$ , i.e., the optimization of the normalized vector  $\mathbf{v}$ , can be given as

$$\mathbf{v} = \frac{\partial_\omega \mathbf{k}(t_p)}{|\partial_\omega \mathbf{k}(t_p)|}, \quad (58)$$

and the quantum Fisher information at  $t_p$  can be obtained as

$$F_Q(t_p) = \frac{(a_1 - a_2)^2 t_p^2 N^2 g^2 \lambda^4 \omega^2 (1 - (\mathbf{m} \cdot \mathbf{n})^2)}{\mu_1^2 \mu_2^2}. \quad (59)$$

Note that this formula only holds at the optimized time points  $t_p$  where the quantum Fisher information is maximized, implying that Eq. (59) can be regarded as the upper envelope of the evolution of quantum Fisher information over time.

It is also noteworthy that as  $\gamma_r(t)$  is independent of the initial state  $|\psi_p\rangle$  of the probe according to Eq. (43), any initial state of the probes can therefore be utilized to achieve the Heisenberg scaling at those time points unless  $\partial_\omega \theta(t_p) = 0$  in which case  $\gamma(t)$  is independent of the parameter  $\omega$  and hence no information about  $\omega$  can be extracted from the evolved state of the ancilla according to Eq. (55).

The above analysis indicates that by selecting appropriate time points and employing the optimal initial states for both the probe system and the ancillary system, the maximum quantum Fisher information can reach the Heisenberg scaling with respect to those time points and the number of probes, although the probes are initially uncorrelated as assumed at the beginning of Sec. IV B.

#### D. Configuration of probe system

We consider the Hamiltonians of the ancillary system to be  $H_a = A = \sigma_z$ . Then the two eigenstates are  $|0\rangle$  and  $|1\rangle$ , and the corresponding eigenvalue of  $A$  are  $a_1 = -a_2 = 1$ . Now the quantum Fisher information at time points  $t_p$  can be written as

$$F_Q(t_p) = \frac{4t_p^2 N^2 g^2 \lambda^4 \omega^2 [1 - (\mathbf{m} \cdot \mathbf{n})^2]}{(g^2 + \lambda^2 \omega^2)^2 - (2g\lambda\omega \mathbf{m} \cdot \mathbf{n})^2}. \quad (60)$$

Here only the quadratic term of  $t_p$  is remained.

It can be verified that the maximum of the quantum Fisher information (60) can be attained when  $\mathbf{m} \cdot \mathbf{n} = 0$  when  $g$  and  $\lambda\omega$  are fixed, implying that non-commuting probe Hamiltonian  $H_p$  and interaction Hamiltonian can increase the estimation precision when the parameter of the probes is indirectly measured via the ancillary system alone, which is consistent with the physical intuition as the interaction Hamiltonian must be non-commuting with the free Hamiltonian of the probe in order to transfer the information of the parameter from the probe to the ancillary system. In this case, the two frequencies coincide,

$$\mu_1 = \mu_2 = \sqrt{g^2 + \lambda^2\omega^2}, \quad (61)$$

which leads to the optimal time points as

$$t_p = 2k\pi/\sqrt{g^2 + \lambda^2\omega^2}, \quad k = 1, 2, 3, \dots, \quad (62)$$

and the maximum quantum Fisher information is

$$F_Q(t_p) = \frac{4t_p^2 N^2 g^2 \lambda^4 \omega^2}{(g^2 + \lambda^2\omega^2)^2}. \quad (63)$$

If the interaction strength  $g$  and the coefficient  $\lambda\omega$  of the probe Hamiltonian are also allowed to be adjusted, the optimization of the quantum Fisher information (60) gives  $g = \lambda\omega$  whenever  $\mathbf{m} \cdot \mathbf{n} \neq \pm 1$ , not necessarily  $\mathbf{m} \cdot \mathbf{n} = 0$ , which imposes a looser constraint on the probe Hamiltonian and the interaction Hamiltonian to achieve the highest precision by measurements on the ancillary system only. The quantum Fisher information at the optimized time points can be found as

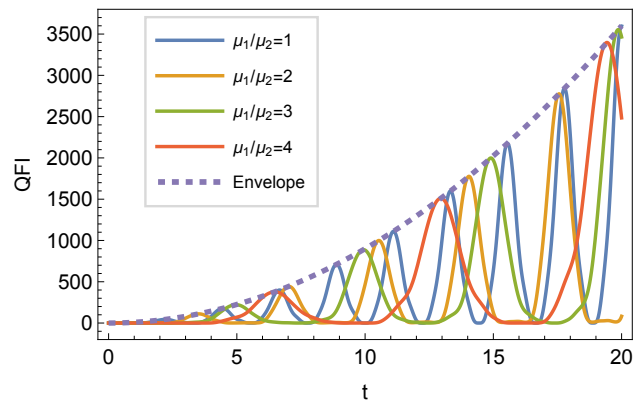
$$F_Q(t_p) = \lambda^2 N^2 t_p^2. \quad (64)$$

If  $\mathbf{m} \cdot \mathbf{n} = \pm 1$ , the argument of  $\gamma(t)$  becomes

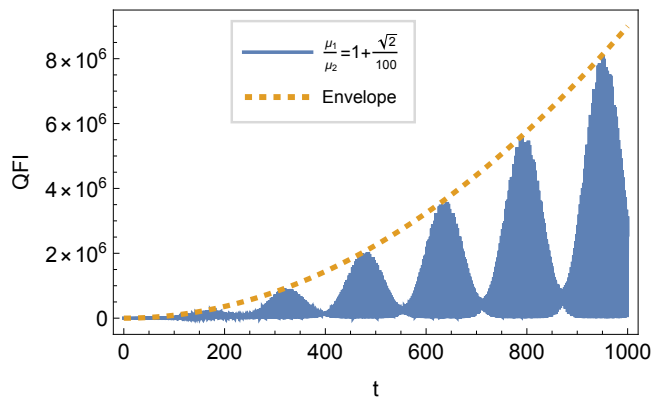
$$\theta(t) = \mp \arctan(\tan(gt) \mathbf{m} \cdot \mathbf{v}), \quad (65)$$

independent of the estimated parameter  $\omega$ , resulting in  $F_Q(t) = 0$  for all time  $t$ , indicating that the Heisenberg scaling cannot be achieved by commuting probe Hamiltonian and interaction Hamiltonian, whatever the interaction strength is.

It is worth noting that in order to achieve the Heisenberg limit of the time scaling of quantum Fisher information, there should always exist time points  $t_p$  satisfying  $\mathbf{k}(t_p) \cdot \mathbf{v} = 1$  with a growing evolution time. Considering  $\mathbf{k}(t_p)$  is composed of sine and cosine functions with two frequencies  $\mu_1$  and  $\mu_2$  while  $\mathbf{v}$  is independent of time, a straightforward approach to satisfy this condition is to choose  $t_p$  as the common period of the two periodic functions, which can be determined by the least common multiples of  $\mu_1^{-1}$  and  $\mu_2^{-1}$  multiplied by a positive integer, so that  $\mathbf{k}(t_p)$  coincides with  $\mathbf{v}$  periodically. If the ratio between the two frequencies  $\mu_1$  and  $\mu_2$  is an integer, the common period is simply the reciprocal of the lower frequency. If the ratio is a rational number, the least common multiple of  $\mu_1^{-1}$  and  $\mu_2^{-1}$  exists and is equal to



(a)



(b)

Figure 2: The quantum Fisher information over the evolution time with the optimal initial state of the probes and the ancillary system and interaction strength  $g = \lambda\omega$  for different ratios of two frequencies  $\mu_1$  and  $\mu_2$ , compared with the same upper envelope given by Eq. (64). (a) The ratio of two frequencies  $\mu_1$  and  $\mu_2$  is rational. (b) The ratio of the two frequencies is irrational.

the reciprocal of the greatest common divisor which can be derived by the Euclidean algorithm. However, if the ratio is an irrational number, an exact common period does not exist and the two cosine functions will never synchronize completely in a regular pattern. But one can always find a rational number to approximate the ratio with an arbitrary precision, and thus derive an approximate common period for the two periodic functions to determine the optimal time points  $t_p$ .

In Fig. 2, the quantum Fisher information is illustrated with the optimal initial states of the probes and the ancillary system and the interaction strength  $g = \lambda\omega$  for different ratios between  $\mu_1$  and  $\mu_2$ , considering both rational and irrational cases for the ratio, and compare them with the upper envelope given by Eq. (64), showcasing the attainability of the same time scaling for the peaks of the quantum Fisher information with different  $\mathbf{m} \cdot \mathbf{n}$  by tuning the interaction strength to  $g = \lambda\omega$  and the time scaling reaches the Heisenberg limit.



## V. CONCLUSIONS

In this work, we propose a protocol that allows uncorrelated probes to surpass the standard quantum limit in parameter estimation by introducing parameter-independent interaction of the probes to external degrees of freedom which serve as an ancillary system. The measurement procedure is simplified by focusing on the ancillary system alone, which is not necessarily the optimal strategy but turns out to be sufficient to achieve the Heisenberg scaling in the precision. The quantum Fisher information exhibits periodic behavior with the evolution time, suggesting that finding appropriate time points is critical to the maximization of the quantum Fisher information. To achieve the highest precision, we perform optimizations of the quantum Fisher information by tailoring the interaction Hamiltonian, choosing proper time points for measurements, and tuning the interaction strength, and finally arrive at the Heisenberg scaling for the estimation precision of parameter in the probe Hamiltonian in terms of both the evolution time and the total probe number.

As a contrast, for a standard measurement protocol to achieve the Heisenberg scaling in the parameter estimation, it typically prepares the probes in an entangled or squeezed state, followed by an encoding unitary evolution process and subsequent measurements on the final state. The outcomes of these measurements are then analyzed to estimate the parameters of interest. However, the utilization of quantum resources is usually challenging in practical applications. The advantage of our protocol is that the Heisenberg scaling can be achieved by a product state of the probes and only the ancilla needs to be measured, which simplifies both the preparation of the initial state and the implementation of the measurement strategy. This simplicity of the protocol may reduce the complexity of realizing Heisenberg-limited precision in experiments and real applications in quantum metrology and other fields.

## ACKNOWLEDGMENTS

This work is supported by the National Natural Science Foundation of China (Grant No. 12075323).

- 
- [1] S. M. Kay, *Fundamentals of statistical signal processing: estimation theory* (Prentice-Hall, Inc., USA, 1993).
  - [2] C. M. Caves, *Physical Review D* **23**, 1693 (1981).
  - [3] D. J. Wineland, J. J. Bollinger, W. M. Itano, F. L. Moore, and D. J. Heinzen, *Physical Review A* **46**, R6797 (1992).
  - [4] V. Giovannetti, S. Lloyd, and L. Maccone, *Nature Photonics* **5**, 222 (2011).
  - [5] G. Tóth and I. Apellaniz, *Journal of Physics A: Mathematical and Theoretical* **47**, 424006 (2014).
  - [6] L. Pezzè, A. Smerzi, M. K. Oberthaler, R. Schmied, and P. Treutlein, *Reviews of Modern Physics* **90**, 035005 (2018).
  - [7] I. Gianani, M. G. Genoni, and M. Barbieri, *IEEE Journal of Selected Topics in Quantum Electronics* **26**, 1 (2020).
  - [8] C. Lee, *Physical Review Letters* **97**, 150402 (2006).
  - [9] F. Albarelli, M. Barbieri, M. G. Genoni, and I. Gianani, *Physics Letters A* **384**, 126311 (2020).
  - [10] R. Demkowicz-Dobrzański, W. Górecki, and M. Guţă, *Journal of Physics A: Mathematical and Theoretical* **53**, 363001 (2020).
  - [11] M. Szczykulska, T. Baumgratz, and A. Datta, *Advances in Physics: X* **1**, 621 (2016).
  - [12] B. C. Nichol, R. Srinivas, D. P. Nadlinger, P. Drmota, D. Main, G. Araneda, C. J. Ballance, and D. M. Lucas, *Nature* **609**, 689 (2022).
  - [13] A. D. Ludlow, M. M. Boyd, J. Ye, E. Peik, and P. O. Schmidt, *Reviews of Modern Physics* **87**, 637 (2015).
  - [14] H. Katori, *Nature Photonics* **5**, 203 (2011).
  - [15] C. M. Caves, *Physical Review D* **23**, 1693 (1981).
  - [16] R. Schnabel, N. Mavalvala, D. E. McClelland, and P. K. Lam, *Nature Communications* **1**, 121 (2010).
  - [17] M. Malnou, D. A. Palken, B. M. Brubaker, L. R. Vale, G. C. Hilton, and K. W. Lehnert, *Physical Review X* **9**, 021023 (2019).
  - [18] S. D. Bass and M. Doser, *Nature Reviews Physics* **6**, 329 (2024).
  - [19] M. A. Taylor and W. P. Bowen, *Physics Reports Quantum metrology and its application in biology*, **615**, 1 (2016).
  - [20] C. A. Pérez-Delgado, M. E. Pearce, and P. Kok, *Physical Review Letters* **109**, 123601 (2012).
  - [21] L. A. Lugiato, A. Gatti, and E. Brambilla, *Journal of Optics B: Quantum and Semiclassical Optics* **4**, S176 (2002).
  - [22] M. Genovese, *Journal of Optics* **18**, 073002 (2016).
  - [23] P.-A. Moreau, E. Toninelli, T. Gregory, and M. J. Padgett, *Nature Reviews Physics* **1**, 367 (2019).
  - [24] C. W. Helstrom, *Journal of Statistical Physics* **1**, 231 (1969).
  - [25] S. L. Braunstein and C. M. Caves, *Physical Review Letters* **72**, 3439 (1994).
  - [26] A. Holevo, *Probabilistic and Statistical Aspects of Quantum Theory* (Edizioni della Normale, Pisa, 2011).
  - [27] V. Giovannetti, S. Lloyd, and L. Maccone, *Physical Review Letters* **96**, 010401 (2006).
  - [28] D. Braun, G. Adesso, F. Benatti, R. Floreanini, U. Marzolino, M. W. Mitchell, and S. Pirandola, *Reviews of Modern Physics* **90**, 035006 (2018).
  - [29] P. C. Humphreys, M. Barbieri, A. Datta, and I. A. Walmsley, *Physical Review Letters* **111**, 070403 (2013).
  - [30] T. Baumgratz and A. Datta, *Physical Review Letters* **116**, 030801 (2016).
  - [31] S. Boixo, S. T. Flammia, C. M. Caves, and J. Geremia, *Physical Review Letters* **98**, 090401 (2007).
  - [32] R. Demkowicz-Dobrzański and L. Maccone, *Physical Review Letters* **113**, 250801 (2014).
  - [33] J. Yang, S. Pang, Z. Chen, A. N. Jordan, and A. del Campo, *Physical Review Letters* **128**, 160505 (2022).
  - [34] S. Pang and A. N. Jordan, *Nature Communications* **8**,

- 14695 (2017).
- [35] J. Liu and H. Yuan, *Physical Review A* **96**, 012117 (2017).
- [36] H. Yuan and C.-H. F. Fung, *Physical Review Letters* **115**, 110401 (2015).
- [37] S. F. Huelga, C. Macchiavello, T. Pellizzari, A. K. Ekert, M. B. Plenio, and J. I. Cirac, *Physical Review Letters* **79**, 3865 (1997).
- [38] J. Kołodyński and R. Demkowicz-Dobrzański, *New Journal of Physics* **15**, 073043 (2013).
- [39] R. Demkowicz-Dobrzański, U. Dorner, B. J. Smith, J. S. Lundeen, W. Wasilewski, K. Banaszek, and I. A. Walmsley, *Physical Review A* **80**, 013825 (2009).
- [40] A. Shaji and C. M. Caves, *Physical Review A* **76**, 032111 (2007).
- [41] B. M. Escher, R. L. de Matos Filho, and L. Davidovich, *Nature Physics* **7**, 406 (2011).
- [42] J. Ma and X. Wang, *Physical Review A* **80**, 012318 (2009).
- [43] P. Hyllus, L. Pezzé, and A. Smerzi, *Physical Review Letters* **105**, 120501 (2010).
- [44] L. A. Rozema, D. H. Mahler, R. Blume-Kohout, and A. M. Steinberg, *Physical Review X* **4**, 041025 (2014).
- [45] O. Hosten, N. J. Engelsen, R. Krishnakumar, and M. A. Kasevich, *Nature* **529**, 505 (2016).
- [46] W.-T. He, H.-Y. Guang, Z.-Y. Li, R.-Q. Deng, N.-N. Zhang, J.-X. Zhao, F.-G. Deng, and Q. Ai, *Physical Review A* **104**, 062429 (2021).
- [47] S. Boixo, A. Datta, S. T. Flammia, A. Shaji, E. Bagan, and C. M. Caves, *Physical Review A* **77**, 012317 (2008).
- [48] G. S. Agarwal and L. Davidovich, *Physical Review Research* **4**, L012014 (2022).
- [49] D. Linnemann, H. Strobel, W. Muessel, J. Schulz, R. J. Lewis-Swan, K. V. Kheruntsyan, and M. K. Oberthaler, *Physical Review Letters* **117**, 013001 (2016).
- [50] S. P. Nolan, S. S. Szigeti, and S. A. Haine, *Physical Review Letters* **119**, 193601 (2017).
- [51] S. Colombo, E. Pedrozo-Peñañiel, A. F. Adiyatullin, Z. Li, E. Mendez, C. Shu, and V. Vuletić, *Nature Physics* **18**, 925 (2022).
- [52] A. W. Chin, S. F. Huelga, and M. B. Plenio, *Physical Review Letters* **109**, 233601 (2012).
- [53] A. Smirne, J. Kołodyński, S. F. Huelga, and R. Demkowicz-Dobrzański, *Physical Review Letters* **116**, 120801 (2016).
- [54] S. Kukita, Y. Matsuzaki, and Y. Kondo, *Physical Review Applied* **16**, 064026 (2021).
- [55] D. Bouwmeester, J.-W. Pan, M. Daniell, H. Weinfurter, and A. Zeilinger, *Physical Review Letters* **82**, 1345 (1999).
- [56] X.-C. Yao, T.-X. Wang, P. Xu, H. Lu, G.-S. Pan, X.-H. Bao, C.-Z. Peng, C.-Y. Lu, Y.-A. Chen, and J.-W. Pan, *Nature Photonics* **6**, 225 (2012).
- [57] Y. Zhong, H.-S. Chang, A. Bienfait, É. Dumur, M.-H. Chou, C. R. Conner, J. Grebel, R. G. Povey, H. Yan, D. I. Schuster, and A. N. Cleland, *Nature* **590**, 571 (2021).
- [58] T. Monz, P. Schindler, J. T. Barreiro, M. Chwalla, D. Nigg, W. A. Coish, M. Harlander, W. Hänsel, M. Hennrich, and R. Blatt, *Physical Review Letters* **106**, 130506 (2011).
- [59] P. Neumann, N. Mizuochi, F. Rempp, P. Hemmer, H. Watanabe, S. Yamasaki, V. Jacques, T. Gaebel, F. Jelezko, and J. Wrachtrup, *Science* **320**, 1326 (2008).
- [60] H. Grote, K. Danzmann, K. L. Dooley, R. Schnabel, J. Slutsky, and H. Vahlbruch, *Physical Review Letters* **110**, 181101 (2013).
- [61] P. Grangier, R. E. Slusher, B. Yurke, and A. LaPorta, *Physical Review Letters* **59**, 2153 (1987).
- [62] T. Xie, Z. Zhao, X. Kong, W. Ma, M. Wang, X. Ye, P. Yu, Z. Yang, S. Xu, P. Wang, Y. Wang, F. Shi, and J. Du, *Science Advances* **7**, eabg9204 (2021).
- [63] C. M. Dawson, A. P. Hines, R. H. McKenzie, and G. J. Milburn, *Physical Review A* **71**, 052321 (2005).
- [64] Z.-H. Wang, B.-S. Wang, and Z.-B. Su, *Physical Review B* **79**, 104428 (2009).
- [65] A. W. Chin, S. F. Huelga, and M. B. Plenio, *Physical Review Letters* **109**, 233601 (2012).
- [66] S. M. Roy and S. L. Braunstein, *Physical Review Letters* **100**, 220501 (2008).
- [67] S. Boixo, A. Datta, M. J. Davis, S. T. Flammia, A. Shaji, and C. M. Caves, *Physical Review Letters* **101**, 040403 (2008).
- [68] M. Napolitano, M. Koschorreck, B. Dubost, N. Behbood, R. J. Sewell, and M. W. Mitchell, *Nature* **471**, 486 (2011).
- [69] Z. Hou, Y. Jin, H. Chen, J.-F. Tang, C.-J. Huang, H. Yuan, G.-Y. Xiang, C.-F. Li, and G.-C. Guo, *Physical Review Letters* **126**, 070503 (2021).
- [70] D. Porras and J. I. Cirac, *Physical Review Letters* **92**, 207901 (2004).
- [71] Y. Lu, S. Zhang, K. Zhang, W. Chen, Y. Shen, J. Zhang, J.-N. Zhang, and K. Kim, *Nature* **572**, 363 (2019).
- [72] J. G. Bohnet, B. C. Sawyer, J. W. Britton, M. L. Wall, A. M. Rey, M. Foss-Feig, and J. J. Bollinger, *Science* **352**, 1297 (2016).
- [73] Z. Yan, Y.-R. Zhang, M. Gong, Y. Wu, Y. Zheng, S. Li, C. Wang, F. Liang, J. Lin, Y. Xu, C. Guo, L. Sun, C.-Z. Peng, K. Xia, H. Deng, H. Rong, J. Q. You, F. Nori, H. Fan, X. Zhu, and J.-W. Pan, *Science* **10.1126/science.aaw1611** (2019).
- [74] C. Song, K. Xu, H. Li, Y.-R. Zhang, X. Zhang, W. Liu, Q. Guo, Z. Wang, W. Ren, J. Hao, H. Feng, H. Fan, D. Zheng, D.-W. Wang, H. Wang, and S.-Y. Zhu, *Science* **10.1126/science.aay0600** (2019).
- [75] P. Roushan, C. Neill, J. Tangpanitanon, V. M. Bastidas, A. Megrant, R. Barends, Y. Chen, Z. Chen, B. Chiaro, A. Dunsworth, A. Fowler, B. Foxen, M. Giustina, E. Jeffrey, J. Kelly, E. Lucero, J. Mutus, M. Neeley, C. Quintana, D. Sank, A. Vainsencher, J. Wenner, T. White, H. Neven, D. G. Angelakis, and J. Martinis, *Science* **10.1126/science.aao1401** (2017).
- [76] Y. Ye, Z.-Y. Ge, Y. Wu, S. Wang, M. Gong, Y.-R. Zhang, Q. Zhu, R. Yang, S. Li, F. Liang, J. Lin, Y. Xu, C. Guo, L. Sun, C. Cheng, N. Ma, Z. Y. Meng, H. Deng, H. Rong, C.-Y. Lu, C.-Z. Peng, H. Fan, X. Zhu, and J.-W. Pan, *Physical Review Letters* **123**, 050502 (2019).
- [77] H. Cramér, *Mathematical methods of statistics.*, Mathematical methods of statistics. (Princeton University Press, Princeton, NJ, US, 1946).
- [78] G. M. D'Ariano, P. Lo Presti, and M. G. A. Paris, *Physical Review Letters* **87**, 270404 (2001).